

TECHNICAL NOTES

Influences of the boundary conditions and linearization on the stability of a radiating fluid in a vertical layer

G. LAURIAT and G. DESRAYAUD

Laboratoire de Thermique, C.N.A.M., 292 rue Saint Martin, 75141 Paris Cedex 03, France

(Received 23 November 1984)

NOMENCLATURE

D	width, $2d$
G	integrated intensity of radiation
n	index of refraction
N	conduction-to-radiation parameter, $\alpha_m \lambda / n^2 \bar{\sigma} T_m^3$
q_r	radiative heat flux
Ra	Rayleigh number based on D , $g\beta \Delta T D^3 / \nu \alpha$
T	temperature
T_m	mean temperature
w	z -component of the velocity.

Greek symbols

α_m	mean extinction coefficient
γ	vertical temperature gradient, $\frac{1}{2} \frac{\partial \theta}{\partial z}$
ΔT	temperature difference between the side walls
ε_i	emissivity of wall i , $i = 1, 2$ at $x = -1, +1$
η	non-grayness factor
λ	thermal conductivity
λ_i	$\lambda_i = \varepsilon_i / (2 - \varepsilon_i)$
σ	complex wave frequency, $\sigma_r + i\sigma_i$
θ	adimensionless temperature, $T/\Delta T$
τ_0	optical thickness, $\alpha_m D$.

Superscript

$-$	base flow quantity.
-----	---------------------

INTRODUCTION

THE EFFECT of radiation on the onset of convection in fluid layers has received considerable attention in the past. However, most of the published studies deal with the Bénard problem and, except in a recent paper [1], it was systematically assumed that the instabilities set in as a stationary mode although the principle of exchange of stabilities has not been shown to hold for this kind of problem. As a consequence of this assumption, the general solution of the linearized stability equations was decomposed into harmonic components with a zero wave speed. Arpaci and Bayazitoglu [2] followed later by Hassab and Özişik [3] have explained that the change over from the conduction regime to the transition regime is expected to occur through a stationary marginal state because the majority of fluid flow problems with pronounced effects of radiation are associated with gaseous media. This result has been proved in many studies for the classical problem of a non-radiative fluid and, in particular, Bergholz [4] has shown clearly that the onset of travelling wave instabilities cannot exist in the conduction regime for low Prandtl numbers ($Pr < 12.7$). Results published recently [1] have confirmed that this assumption is still valid for symmetric radiative boundary

conditions (two black, two mirror or two identical gray surfaces) and if the non-linear term contained in the radiation equation for the base flow is linearized. In these cases, in fact, the odd symmetry of the base flow solution is retained. On the other hand, for cases with asymmetric boundary conditions [3, 5], this property is destroyed and there is no proof that the principle of exchange of stabilities holds. Such situations are encountered in various problems, for example in the presence of a density extremum or for flows between vertical concentric cylinders where the odd symmetry of the velocity profile no longer exists. It appears then that the flow undergoes a transition to multicellular unsteady patterns [6, 7].

In the present work the emphasis is on the influence of asymmetric boundary conditions and non-linear terms in the radiation equation on the stability of the conduction, transition and boundary-layer regimes. A vertical layer of a radiating fluid contained between two parallel plates maintained at uniform but different temperatures is studied.

ANALYSIS

In the model considered, the axes x and z are chosen to be normal and along the sides of a vertical narrow gap of width $2d$ and the origin is in the middle plane. The fluid has a kinematic viscosity ν , a thermal diffusivity α , a coefficient of thermal expansion β and the Boussinesq approximation is invoked. The radiation part is solved using the $P-1$ approximation modified to allow for the non-grayness effects [3].

The governing equations are made dimensionless by scaling length, velocity and temperature with d , $g\beta\Delta T d^2/\nu$ and ΔT while the radiative flux q_r and the integrated intensity of radiation G are non-dimensionalized by $n^2 \bar{\sigma} T_m^3 \Delta T$. Neglecting the radiative contributions to momentum and making the classical assumptions of one-dimensional base flow [4, 8], the equations governing the initial steady motion are given by

$$\frac{d^2 \bar{w}}{dx^2} + \bar{\theta} = C \quad (1)$$

$$\frac{m^4}{4} \bar{w} - \frac{d^2 \bar{\theta}}{dx^2} + \frac{\tau_0}{2N} \frac{d\bar{q}_r}{dx} = 0 \quad (2)$$

$$\frac{d^2 \bar{q}_r}{dx^2} - \frac{3\tau_0}{4} \bar{q}_r - \frac{2\tau_0 \eta}{\bar{\theta}_m^3} \frac{d\bar{\theta}^4}{dx} = 0 \quad (3)$$

where the parameter m defined as in [4] characterizes the vertical temperature stratification.

The boundary conditions at $x = \pm 1$ are

$$\bar{w} = 0 \quad (4)$$

$$\bar{\theta} = \bar{\theta}_m \pm 0.5 \quad (5)$$

$$\bar{q}_r \pm 2 \frac{\lambda_i}{\eta \tau_0} \frac{d\bar{q}_r}{dx} = 0. \quad (6)$$

The constant appearing in equation (1) is determined by a

	m	1.0	3.0	4.5	5.0	6.25	7.0	9.0	12.0
Linear	$\bar{w}_{\max} \times 10^3$	6.28	5.63	4.03	3.44	2.27	1.80	1.08	0.59
	Gr_c	11 328	14 482	53 205	279 062	411 101	242 395	349 772	793 651
	α_c	2.55	2.42	1.48	1.28	1.50	3.01	4.21	5.56
	$c \times 10^3$	0.0	0.0	0.0	0.0	± 1.08	± 1.00	± 0.658	± 0.376
Non-linear	Gr_c	11 414	14 582	51 761	234 113	253 627	216 503	332 614	762 869
	α_c	2.55	2.41	1.53	1.28	2.05	3.07	4.24	5.60
	$c \times 10^3$	-0.137	-0.141	-0.213	-0.358	-1.10	-1.01	-0.668	-0.380

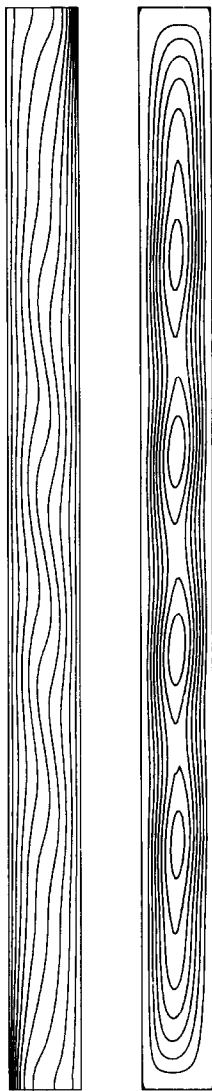


FIG. 1. Steady streamlines and isothermal patterns ($A = 15$, $Gr = 15\,000$, $Pr = 0.72$, $\varepsilon_1 = \varepsilon_2 = 1$, $\tau_0 = 1$, $N = 0.5$).

Computations were then performed without using the linear approximation and, on account of the value of c reported in Table 1, a wave motion with low frequency was expected. The results are shown in Fig. 2 where streamlines are plotted for a full period covered within 720 time steps. The cells are formed at the top of the cavity and they drift downward with a speed of $c = 1.51 \times 10^{-4}$ and a wave number calculated from the central cell to be 2.32. These values differ only 6.7% and 3.8% from the critical values.

Next the effects of a dissymmetry of the radiative properties of the isothermal walls are investigated. In a slot with a black cold wall, a decrease of the emissivity of the hot wall produces a decrease of the temperatures in the core while increases of the temperature gradients and of the vertical velocities occur near the hot wall. Indeed conduction and convection compensate for the weakening of radiation at the reflecting wall [10]. Reversed effects are shown by decreasing the emissivity of the cold wall with a black hot wall. Consequently, the odd symmetry of the temperature distribution is destroyed.

Results of the stability analysis with a linearized radiation term are reported in Table 2. For the set of parameters considered, the critical Grashof numbers are within a few percent the values given by Hassab and Özişik [3]. As shown, the decrease of the emissivities stabilizes the flow with a stronger effect as the interaction parameter is reduced. A zero wave speed is obtained for identical emissivities while small wave speeds are calculated as soon as the radiative boundary conditions differ. The wave speeds are negative for an emissivity of the cold wall lower than the emissivity of the hot wall whereas the opposite is true in the reversed case. Therefore, in a vertical layer of radiating fluid, the mechanism for the onset of instability in the conduction regime depends on the specific values of the emissivities: the instability sets in as a stationary multicellular mode for $\varepsilon_1 = \varepsilon_2$ while a travelling mode with a single wave is found for $\varepsilon_1 \neq \varepsilon_2$. The wave moves upward when the emissivity ε_1 of the cold wall is greater than ε_2 and downward in the case $\varepsilon_1 < \varepsilon_2$. These results can be related to those obtained recently [7, 8, 11] showing the effect of curvature on the stability of the conduction regime in a tall vertical annulus: the wave moves in the direction of the higher base flow velocity for fluids having low Prandtl numbers.

The problem becomes more complicated when the radiative term is not linearized because the highest velocities do not occur systematically near the reflecting wall. For example, when considering again the previous set of radiative parameters, the maximum base flow velocities are always located near the cold wall if it is the more reflective wall. It was found then that the wave moves downward as shown in Table

Table 2. Critical Grashof number, wave number and wave speed in the conduction regime

			$N = 4$			$N = 0.4$		
	ε_1	ε_2	$\eta = 0.4$	$\eta = 1$	$\eta = 4$	$\eta = 0.4$	$\eta = 1$	$\eta = 4$
Gr_c	1	1	8 292	8 952	12 630	8 959	10 765	19 224
α			2.78	2.73	2.54	2.66	2.60	2.59
Gr_c	0	1	8 590	9 500	13 820	12 051	16 049	28 269
α			2.77	2.70	2.50	2.56	2.46	2.50
$c \times 10^4$			-0.632	-0.899	-0.818	-2.19	-1.53	-0.299
Gr_c	1	0	8 585	9 498	13 828	12 074	16 130	28 277
α			2.77	2.70	2.50	2.56	2.46	2.50
$c \times 10^4$			+0.621	+0.901	+0.819	+2.21	+1.55	+0.315
Gr_c	0	0	8 863	10 014	15 001	15 009	21 430	37 171
α			2.75	2.68	2.46	2.46	2.35	2.42

$m = 0, \tau_0 = 2.0, Pr = 0.72.$

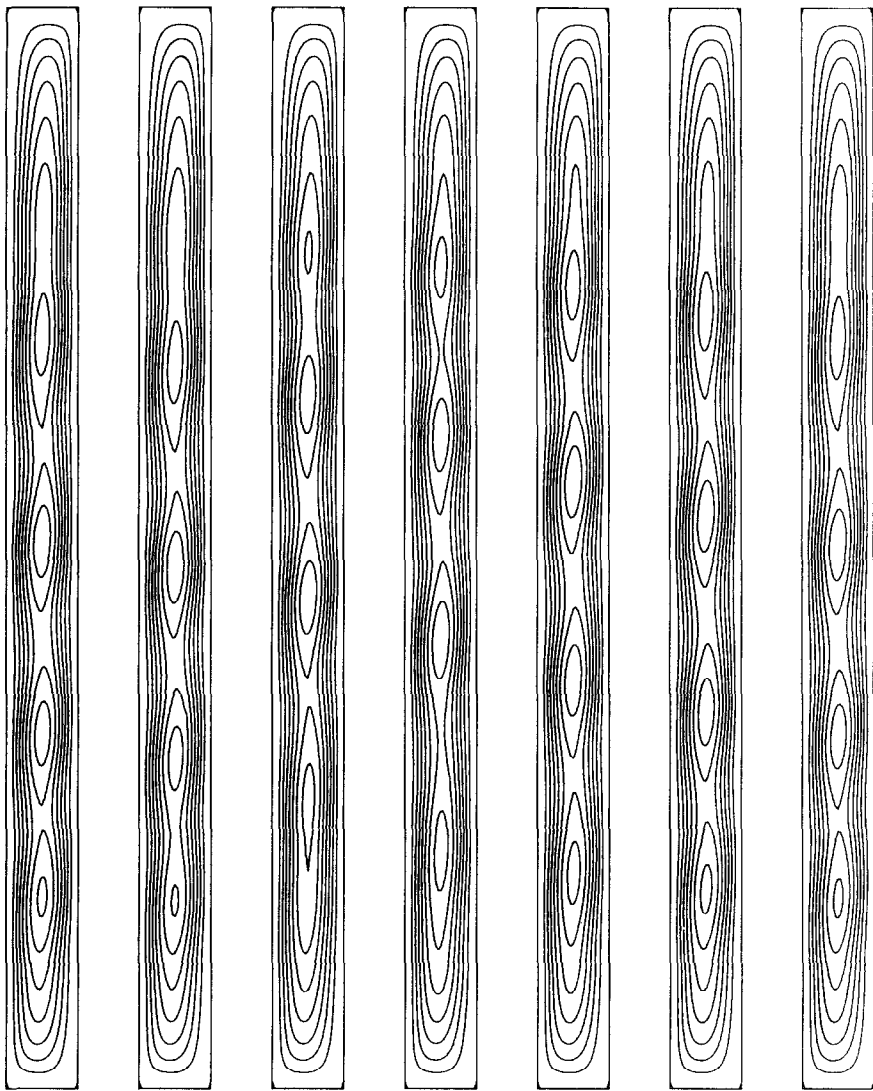


FIG. 2. Streamlines patterns of the unsteady multicellular motion over one period (same parameters as in Fig. 1).

Table 3. Influences of the wall emissivities on the critical values

(a)						(b)					
ε_1	ε_2	Gr_c	α_c	$c \times 10^3$	$\bar{w}_{max} \times 10^3$	ε_1	ε_2	Gr_c	α_c	$c \times 10^3$	$\bar{w}_{max} \times 10^3$
1	1	10932	2.59	−0.106	−5.90	1	0.75	11539	2.57	−0.078	−5.65
0.75	1	11799	2.56	−0.128	−5.57	1	0.5	12367	2.55	−0.042	−5.35
0.5	1	12950	2.54	−0.151	−5.21	1	0.25	13574	2.52	−0.005	−4.98
0.25	1	14561	2.50	−0.181	−4.79	1	0	15522	2.47	+0.070	+4.54
0	1	17066	2.43	−0.219	−4.32	0.75	0	16418	2.45	+0.045	+4.37
0	0.75	17600	2.42	−0.199	−4.22	0.5	0	17610	2.43	+0.015	−4.17
0	0.5	18422	2.41	−0.169	−4.09	0.25	0	19160	2.39	−0.022	−3.94
0	0.25	19634	2.38	−0.130	−3.92						
0	0	21613	2.32	−0.072	−3.68						

$N = 0.4, \tau_0 = 2, \eta = 1, m = 1, Pr = 0.72.$

3(a) for selected couples of emissivities. If we consider now the reversal [Table 3(b)], the maximum velocities can be obtained either near the cold wall or near the hot wall according to the values of the difference ($\varepsilon_1 - \varepsilon_2$). The dominant wave then moves upward or downward. Therefore, the behavior of the flow *vis-à-vis* the disturbances cannot be predicted unlike when using the linear approximation.

The results of the stability analysis were complemented by some numerical simulations in order to have other information about the structure of the flow. There again, the computations are in agreement with the theoretical findings regarding both the stabilizing effect shown in Table 2 and the motion of the cells depicted previously (critical wave numbers and wave speeds). What is learnt from the simulations in a slot of finite aspect ratio is that the instability develops locally: from the streamline patterns plotted for one of the extreme cases ($\varepsilon_1 = 0, \varepsilon_2 = 1$), the cells are seen in the lower half part of the cavity and for the other ($\varepsilon_1 = 1, \varepsilon_2 = 0$), the cells are in the upper part. These patterns show that the dominant travelling wave fills the end of the cavity. However, as seen from the distribution of the stream function in the central middle plane, the cells due to this kind of dissymmetry are weak at the onset of instability (variations of the streamfunction within 5% at $Gr = 16000$ for the case shown in Table 2). Finally the analogy between the present results and those obtained in a fluid contained in a vertical annulus [11, 12] must be emphasized again. Since streamlines patterns are not shown in this paper due to space limitation, the reader could find similar pictures of the effects of a reflecting hot wall by referring to the paper of Lee *et al.* [11] in which the inner cylinder is hot. The case of a reflecting cold wall corresponds to an outer hot cylinder.

CONCLUSION

Linear stability theory is used to study the conditions marking the onset of convective instabilities in vertical layers of radiating fluids. The calculations are done without linearizing the radiation term in the base flow equations and for dissimilar radiative boundary conditions. In the conduction and transition regimes, the results show that the instabilities set in as a single travelling wave whose moving direction is strongly dependent on the emissivities of the bounding walls. For higher stratification parameters, one of the two oppositely travelling waves which are seen for symmetric base flows dies out. The multicellular structures of

flows obtained by numerical integration of the equation governing the motion in a slender cavity are found to be in agreement with the predictions of the stability theory.

REFERENCES

1. G. Desrayaud and G. Lauriat, On the stability of natural convection of a radiating fluid in a vertical slot, *Int. Commun. Heat Mass Transfer* **11**, 439–450 (1984).
2. V. S. Arpaci and Y. Bayazitoglu, Thermal stability of radiating fluids: asymmetric slot problem, *Phys. Fluids* **16**, 589–593 (1973).
3. M. A. Hassab and M. N. Özışık, Effects of radiation and convective boundary conditions on the stability of fluid in an inclined slender slot, *Int. J. Heat Mass Transfer* **22**, 1095–1105 (1979).
4. R. F. Bergholz, Instability of steady natural convection in a vertical fluid layer, *J. Fluid Mech.* **84**, 743–768 (1978).
5. V. S. Arpaci and D. Gözümlü, Thermal instability of radiating fluids: the Bénard problem, *Phys. Fluids* **16**, 581–588 (1973).
6. A. M. Shaaban and M. N. Özışık, The effect of nonlinear density stratification on the stability of a vertical water layer in the conduction regime, *Trans. Am. Soc. mech. Engrs, J. Heat Transfer* **105**, 130–137 (1983).
7. A. M. Shaaban and M. N. Özışık, Effect of curvature on the thermal stability of a fluid between two vertical coaxial cylinders, *Proc. 7th Int. Conference Heat and Mass Transfer*, Vol. 2, NC 27, pp. 281–286 (1982).
8. C. M. Vest and V. S. Arpaci, Stability of natural convection in a vertical slot, *J. Fluid Mech.* **36**, 1–16 (1969).
9. G. Desrayaud and G. Lauriat, Natural convection of a radiating fluid in a vertical layer, *J. Heat Transfer* (in press).
10. G. Lauriat, Combined radiation–convection in gray fluids enclosed in vertical cavities, *J. Heat Transfer* **104**, 609–615 (1982).
11. Y. Lee, S. A. Korpela and R. N. Horne, Structure of multicellular natural convection in tall vertical annulus, *Proc. 7th Int. Conference Heat and Mass Transfer*, Vol. 2, NC 17, pp. 221–226 (1982).
12. I. G. Choi and S. A. Korpela, Stability of the conduction regime of natural convection in a tall vertical annulus, *J. Fluid Mech.* **99**, 725–738 (1980).

Parameterization of system behavior for salt-stratified solutions heated from below with and without salinity-maintained mixed layers

T. L. BERGMAN, F. P. INCROPERA and R. VISKANTA

Heat Transfer Laboratory, School of Mechanical Engineering, Purdue University, West Lafayette, IN 47907, U.S.A.

NOMENCLATURE

C	constant
c_v	specific heat
g	gravitational acceleration
k	thermal conductivity
L	arbitrary length
m_s	salt mass fraction
q_b	applied bottom heat flux
Ra_s^*	solutal Rayleigh number, $g\beta_s(dm_s/dz)_i L^4/\alpha v$
Ra_T^*	modified thermal Rayleigh number, $g\beta_T q_b L^4/k\alpha v$

T	temperature
t	time
X	ratio of modified thermal Rayleigh number to solutal Rayleigh number
Y	dimensionless parameter, $(dm_s/dz)_i(X\alpha t)^{1/2}/m_{s,0}$
z	vertical space coordinate positive upward.

Greek symbols

α	thermal diffusivity, $k/(\rho c_v)$
β_s	solutal expansion coefficient, $\rho^{-1} \partial \rho / \partial m_s _T$
β_T	thermal expansion coefficient, $\rho^{-1} \partial \rho / \partial T _{m_s}$